International Journal of Heat and Mass Transfer 103 (2016) 1058–1064

Contents lists available at ScienceDirect

International Journal of Heat and Mass Transfer

journal homepage: www.elsevier.com/locate/ijhmt

Molecular dynamics study on thermal transport at carbon nanotube interface junctions: Effects of mechanical force and chemical functionalization

Wen Chen [a], Jingchao Zhang [b,*], Yanan Yue [a,*]

[a] School of Power and Mechanical Engineering, Wuhan University, Wuhan, Hubei 430072, China
[b] Holland Computing Center, University of Nebraska-Lincoln, Lincoln, NE 68588, USA

ARTICLE INFO

Article history:
Received 12 May 2016
Received in revised form 7 August 2016
Accepted 9 August 2016

Keywords:
Molecular dynamics
Interface thermal conductance
Carbon nanotube
Modulation

ABSTRACT

Classical molecular dynamics (MD) simulations are performed in this work to investigate the interfacial thermal transport across stacked carbon nanotube (CNT) junctions. Various approaches are implemented to increase the thermal conductance (G) between CNTs. Effects of crossing angle, contact area, bonding strength, external force and hydrocarbon functionalization on G are investigated. A remarkably increase of thermal conductance is achieved by connecting two CNTs with hydrocarbon chain linkers CH_2. The predicted G changes from 229 pW/K without linkers to 4901 pW/K with an optimized linker number, which increases by a factor of 20. Meanwhile, thermal conductance is found to increase monotonically with contact area but decrease inversely with crossing angle. The van der Waals (*vdW*) bonding strength has similar effects with applied external force on thermal conductance, both of which facilitate the interfacial thermal transport by enhancing the contact pressures. Synthesized relationship of internal coupling strength, external force and final separation distance between CNTs is explored to illustrate the variation of thermal conductance and intermolecular potential energy.

1. Introduction

Carbon nanotubes (CNTs) have been regarded as one of the perfect materials for improving heat transfer performance since their first discovery [1]. The axial thermal conductivity (κ) of individual CNT can reach a very high level beyond 3000 W/m·K from previous work [2]. The remarkable thermal conductivity is partially attributed to the intrinsic well-organized geometric construction and highly stiff C–C sp^2 atomic bonds. With ever-increasing applications in thermal management due to their superb thermal properties [3–5], studies on the heat transfer processes of CNT-based composite materials are urgently needed. Although κ of single CNT is extremely high, significant decreases of κ are reported in CNT-based composite materials and CNT bulk materials [6–8]. The high thermal resistance at CNT interfaces is one of the major factors hindering its thermal performance [9–11]. To facilitate thermal transport between CNTs, the heat transfer mechanism across CNT-CNT interfaces needs to be comprehensively explored.

The Kapitza conductance, known as Kapitza resistance or interfacial thermal resistance [12], is defined as $G = q/\Delta T$, where G, q and ΔT correspond to Kapitza conductance, heat flux rate and temperature drop, respectively. There have been various methods for investigating the CNT-CNT interfacial thermal conductance. Zhong et al. [13] modeled a non-stationary heat transfer process between two parallel 5 nm long (10,10) carbon nanotubes with 2.5 nm overlap and 6 Å separation distance using molecular dynamics (MD) simulations. The predicted G between the two carbon nanotubes was around 13 pW/K. Xu et al. [14] studied the parallel single wall carbon nanotubes (SWCNTs) by making a nanotube overlapped with two other nanotubes at both ends and obtained the thermal conductance around 100–1000 pW/K based on different overlap length. Two approaches, *i.e.*, phonon spectrum matching and interfacial coupling, were developed to improve the interfacial thermal conductance. A method for phonon spectrum matching is using materials with similar phonon spectrum at interface. It was reported that the increase of contact length between CNTs, polymer-wrapped CNT interface and a metal layer coating on CNTs can enhance the coupling strength by Xu et al. [14]. Chalopin et al. [15] calculated the partial thermal conductance at the junction and their dependence with chirality at different temperatures using the Green's function. The calculated G varied from 10 pW/K to 100 pW/K at temperature 300 K. Yang et al. [16] measured G in two cases. One is about the cross junction between two

* Corresponding authors.
E-mail addresses: zhang@unl.edu (J. Zhang), yyue@whu.edu.cn (Y. Yue).

http://dx.doi.org/10.1016/j.ijheatmasstransfer.2016.08.016
0017-9310/

Nomenclature

G	thermal conductance, pW/K
q	heat flux rate, W
ΔT	temperature drop, K
T	temperature, K
n	number of atoms
k_B	Boltzmann constant, J/K
m	mass, kg
E	potential energy, J
V	potential energy, J
r	interatomic distance, Å
L	length, mm
D	diameter, nm
G'	actual thermal conductance, pW/K
d	interlayer distance, Å

Greek symbols

v	velocity, m/s
χ	scaling parameter
ε	energy parameter, eV
θ	angle, degree
σ	van der Waals diameter, Å
λ	ratio of thermal conductance

Subscripts

k,i,j,l	serial number of atom

multiwalled CNTs with diameters of 74 nm and 121 nm, and the thermal conductance was in the order of 10^4 pW/K; the other one is parallel aligned with 2.6 μm in contact length between two multiwalled CNTs with diameters of 170 nm and 165–185 nm, and the thermal conductance was about 10^6 pW/K which was two orders of magnitude higher than that in the former case. Foygel et al. [17] theoretically predicted the thermal conductance in the order of 10^4–10^5 pW/K.

Strengthening the interactions between two CNTs is an effective way to facilitate the CNT-CNT interfacial thermal transport. It can be achieved by increasing thermal contact area (A) [18], applying external force [19] or using chemical organic linkers to connect two individual CNTs [20]. Varying thermal contact angle between two CNTs is feasible to regulate thermal contact area, and thus modulate interfacial thermal transport. Hu et al. [18] simulated two (6,6) single-walled CNTs with different crossing angles from 0° to 90° for different tube lengths of 90 nm and 120 nm using MD simulations. They found that G had an inverse dependence of crossing angle. Smaller thermal contact angle corresponds to a larger A which means better thermal interaction and larger interfacial thermal conductance. Evans et al. [19] also investigated the effect of junction area on interfacial thermal conductance by varying the crossing angles from 0° to 90° and the effect of force applied in the cross-plane direction which is perpendicular to the tube axes on thermal conductance with two limiting crossing angles (0° and 90°) using MD simulations. The effect of junction area/crossing angle on thermal conductance had the same tendency as shown in the work by Hu et al. [18]. The effect of applied force on thermal conductance is twofold reported by Evans et al. [19]. On the one hand, applied force reinforces the CNT-CNT van der Waals (*vdW*) bonding to increase interfacial thermal conductance; on the other hand, applied force deforms the CNTs to alter the junction area between CNTs which may increase or decrease thermal conductance according to different crossing angles. Varshney et al. [20] developed a range of two-nanotube-linked models which consist of two CNTs linked with different chemical organic molecules immersed in the epoxy matrix using MD simulations. The effects of linker type and linker number on thermal conductance were explored [20]. It was reported that there was a positive correlation between G and the number of linkers and an inverse dependence of G on the length of linkers between CNTs in their work. The increased number of covalent bonds due to condensed linkers would reinforce thermal transport between CNTs. They found that longer linkers would increase the separation distance between CNTs, which would weaken the *vdW* interaction and reduce the G values. However, the increasing trend of G with linker amount was only confirmed at very small scales, and whether the trend will continue as the number of linker increases is an unknown problem.

Despite of the existing studies on the thermal conductance across CNT interfaces, the heat transfer mechanisms in aspects of contact angle/area, internal/external pressures and large amount of chemical linkers are still unclear. In this work, effects of crossing angle on CNT-CNT thermal conductance are comparatively studied with thermal contact area. Besides, modulations of interfacial thermal conductance by different interaction types, such as the internal coupling strength, external exerted force and the covalent hydrocarbon functionalization, are systematically investigated. In addition, the size effect of CNTs on G is significant and there have been works about the size effect on G between CNTs. Evans et al. [19] investigated effect of CNT length on contact conductance and found a positive dependence of thermal conductance on CNT length. In their work, thermal conductance reached saturation of 91 pW/K for CNT length of 20 nm. Hu et al. [18] and Salaway et al. [21] both explored CNT length effect on thermal conductance between two perpendicular CNTs with lengths ranging from 20 to 200 nm. The trends of thermal conductance varied with CNT length are coincident with that in the work by Evans et al. [19], whereas thermal conductance neither seemed to be saturated even CNT length reached 200 nm.

2. Models, physical basis, and computational approach

In this work, non-equilibrium molecular dynamics (NEMD) [22] is applied to investigate the CNT-CNT interfacial thermal conductance. Two 10 nm length (10,10) CNTs are used in all simulations. Atomic configuration of the hybrid system is shown in Fig. 1. To build a constant temperature gradient, 200 atoms at each end of one CNT are grouped as hot reservoirs with a heat flux rate q by velocity rescaling, and 200 atoms at each end of the other CNT are treated as the cold reservoirs with negative q. The amount of thermal energies added/subtracted to/from the hot/cold reservoirs are equivalent, which ensures the overall temperature of the system remains constant. Only non-translational kinetic energies are applied in the thermal reservoirs so the system's aggregate momentum is conserved. The outermost 20 carbon atoms at each end of both CNTs are fixed to prevent the CNTs from moving and rotating [23]. The remaining regions are divided into 10 slabs along the transverse direction. The temperature of each slab is calculated as

$$T = \frac{1}{3nk_B}\sum_{k=1}^{n} m_k v_k^2 \tag{1}$$

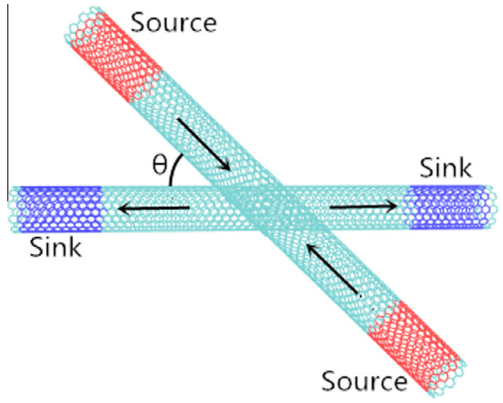

Fig. 1. Atomic configuration of two stacking CNTs with different contact angle θ. The red and blue regions denote heat source and heat sink respectively. The black arrows represent the heat flux directions. (For interpretation of the references to colour in this figure legend, the reader is referred to the web version of this article.)

where n is the number of atoms in each slab, k_B is the Boltzmann constant, m_k and v_k are the atomic mass and velocity of atom k, respectively. The temperature drop ΔT at the interface can be used to calculate the thermal conductance. The adaptive intermolecular reactive empirical bond-order (AIREBO) potential [24] is used to describe the C–C and C–H interactions within each CNT and hydrocarbon linkers. The 12–6 Lennard Jones (LJ) potential [25] is adopted to model the interactions between different CNTs. The AIREBO potential E (refers to potential energy for REBO potential) is described as

$$E = \frac{1}{2}\sum_{i}\sum_{j\neq i}\left[E_{ij}^{\mathrm{REBO}} + E_{ij}^{\mathrm{LJ}} + \sum_{k\neq i,j}\sum_{l\neq i,j,k} E_{kijl}^{\mathrm{TORSION}}\right] \tag{2}$$

where the E^{REBO} term describes short-ranged C–C, H–H and C–H interactions; the E^{LJ} describes long-ranged interactions and the E^{TORSION} term is an explicit 4-body potential that describes various dihedral angle preferences in hydrocarbon configurations. In this paper, both E^{LJ} and E^{TORSION} are turned off in order to study the effect of interaction strength on thermal conductance since the LJ potential is convenient to be adjusted as Eq. (3). The 12–6 Lennard Jones (LJ) potential V (refers to potential energy for LJ potential) is expressed as

$$V(r) = 4\chi\varepsilon\left[\left(\frac{\sigma}{r}\right)^{12} - \left(\frac{\sigma}{r}\right)^{6}\right] \tag{3}$$

where r is the interatomic distance; $\varepsilon = 2.84$ meV is the energy parameter, and $\sigma = 3.4$ Å is the *vdW* diameter. The scaling parameter χ is used to adjust the interaction strength between CNTs. But it is impossible to tune the *vdW* bonding strength by changing scaling parameter χ directly in reality. All simulations are performed using the LAMMPS molecular dynamics package [26].

As shown in Fig. 1, the thermal junction is located at the absolute geometrical middle of each CNTs. To study the crossing angle's (θ) effect on thermal conductance, θ between the axes of the stacked CNTs is varied from 0° to 90°. The red regions and blue regions represent the heat source and heat sink, respectively. The initial separation distance, which is defined as the nearest distance between the outer walls of opposing CNTs at the junction, is set as 3 Å for all studies. The system is initially equilibrated at temperature 300 K for 200 ps (1 ps = 10^{-12} s) using a Nose–Hoover thermostat [27] with an integration step of 0.2 fs (1 fs = 10^{-15} s). A consecutive micro-canonical ensemble (NVE) is followed for another 400 ps. Finally, a constant heat flux rate q is applied to the system for another 7×10^6 time steps to reach steady state. For a given thermal conductance, larger heat flux rates lead to significant temperature drops which could cause non-linear effect, while lower fluxes lead to reduced temperature drops which could lead to severer statistical uncertainties due to unexpected temperature fluctuations [19]. To reach the same level of temperature differences, the applied heat flux rates are adjusted from 1.6 nW to 2.4 nW for different structures. This magnitude of heat flux rate is used to create a statistically significant but not excessive temperature drop between the CNTs.

Two orthogonal stacked ($\theta = 90°$) CNTs are further investigated to analyze the effect of *vdW* bonding strength on thermal conductance. The MD system configuration, simulation process and heat flux rate are the same as those in previous calculations. An artificial scaling factor χ in Eq. (3) is used to adjust the strength of *vdW* bonding between CNTs. The scaling factor χ is varied from 0.2 to 2. The same system is selected to study the effect of applied external force on thermal conductance. The force is evenly distributed in the normal direction of each nanotube as shown in Fig. 2. It is worth noting that the magnitude of applied force needs to be carefully adjusted since the CNT structure may collapse if the applied force is too large.

Hydrocarbon chain linkers CH_2 are selected to connect two parallel CNTs to study the effect of chemical functionalization on thermal conductance. The structure diagram of five linkers is displayed in Fig. 3. As many as 35 linkers are constructed between two CNTs considering the separation distance between adjacent linkers. If the number of linkers is superabundant, adjacent linkers will be too close and covalent bonds will form between adjacent linkers. In this case, the CNT-CNT interfacial thermal conductance enhances heavily, so the heat fluxes applied are much larger than those in former cases. The heat flux rates are varied from 16 nW to 100 nW according to different number of linkers in order to create an appropriate temperature drop ΔT between two CNTs.

3. Results and discussion

3.1. Effects of crossing angle and contact area

The thermal conductance as a function of crossing angle and contact area is shown in Fig. 4. The thermal contact area is calculated as $A = D^2/\sin\theta$, where D and θ are the diameter of the CNT and crossing angle between CNTs, respectively [18]. Although the CNTs contact in a point or a line, the interaction between two CNTs is in an area considering interatomic interaction. And the junction area is regarded quantitatively as projected area in the in-plane and calculated as $A = D^2/\sin\theta$. It is observed that the thermal conductance has a positive correlation with A and a negative correlation with θ, which were also confirmed by previous numerical studies [18,19]. With larger A and smaller θ, more carbon atoms

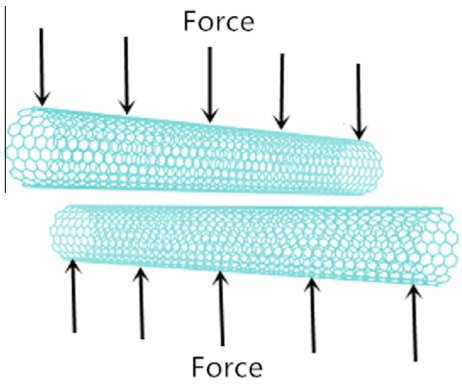

Fig. 2. Structure diagram of two perpendicular CNTs applied with external force. The forces are exerted in the normal directions and evenly distributed along the nanotubes. The arrows represent the force directions.

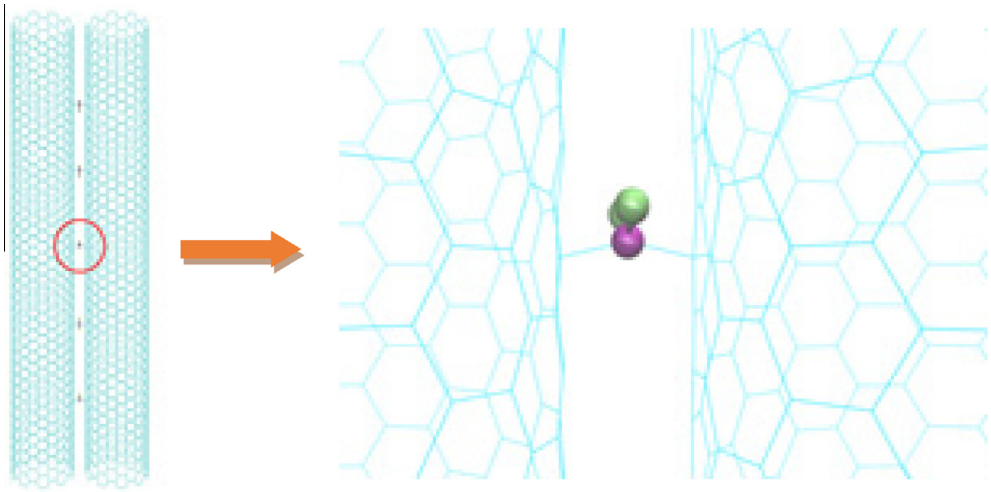

Fig. 3. Atomic configuration of two parallel CNTs connected with hydrocarbon CH_2 chain linkers. The left diagram depicts the integral structure; the right diagram shows the enlarged picture for a specific linker.

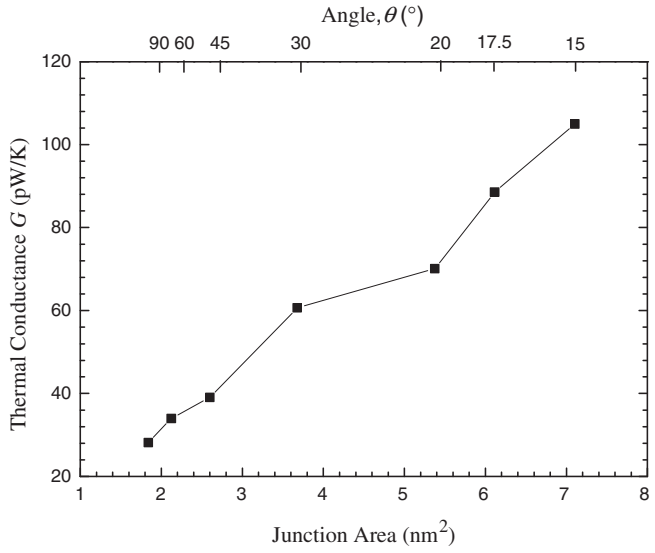

Fig. 4. Thermal conductance as a function of crossing angle θ and junction area. The junction area is calculated as $D^2/\sin\theta$.

from both sides of the junctions are involved in the thermal transport process and start contributing to the heat dissipation across the boundary, which directly enhance the interfacial thermal conductance and results in greater G values.

Evans et al. [19] calculated the thermal conductance of (10,10) CNTs of lengths 20 nm at ~75 pW/K with crossing angle 90°, which is higher than 28 pW/K in our work. It is noted that they used longer CNTs of 20 nm compared to 10 nm CNTs in our work considering the effect of tube length on thermal conductance [28,29] and they used stronger LJ interactional energy scale $\varepsilon = 3$ meV in their work compared to $\varepsilon = 2.84$ meV in our work. Hu et al. [18] derived the thermal conductance of 90 nm long (6,6) CNTs with crossing angle 90° was about 40 pW/K; it's much closer to our predicted result. The experimental measurement by Yang et al. [16] reported the G of cross contacted multi-walled CNTs with diameters of 74 nm and 121 nm was at the range of 10^4 pW/K which is much higher than values of numerical results. The deviation between experimental observations and MD simulation results is very common, especially in thermal transport study of low-dimensional materials [30,31]. As per our study, there are two possible reasons: (1) The junction between CNTs in MD simulation is set as a perfect structure, whereas in real experiment, the contact could be in different form and it is hardly to characterize. As to MD simulations, potential functions describing interatomic and intermolecular interaction can be easily defined while the actual interatomic interaction and intermolecular interaction in experiment may be difficult to define. (2) Besides the effect of sample quality, different experimental setup could give different conductance values. It can be from the characterization temperature, stability of heating sources and many other factors. However, the simulation processes are quite similar and results are consistent in MD simulations.

3.2. Effects of interaction strength and external force

Dependence of G on LJ scaling parameter χ is shown in Fig. 5. The monotonic increasing trend indicates that the phonon couplings between two CNTs are enhanced when χ becomes larger, which will strengthen the heat conduction between two CNTs. Previous works studied the effects of coupling strength χ on thermal conductance between graphene nanoribbon (GNR) and hexagonal boron-nitride nanoribbon (h-BN) by Zhang et al. [32] and between

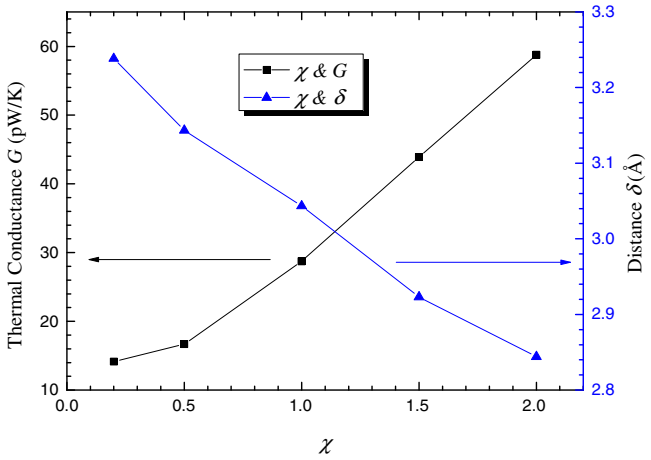

Fig. 5. Synthesized relationship of LJ parameter χ, thermal conductance G and final separation distance δ. The black solid line with square symbols represent χ as a function of G, and the blue solid line with uptriangle symbols describes χ as a function of δ. (For interpretation of the references to colour in this figure legend, the reader is referred to the web version of this article.)

two GNRs by Xu et al. [14]. A new parameter λ is defined as $\lambda = G_{\chi=2}/G_{\chi=0.5}$ where $G_{\chi=2}$ and $G_{\chi=0.5}$ are thermal conductance when χ equals to 2 and 0.5, respectively. The parameter λ equals ~3.6 in our work, while λ = ~2.3 at temperature 300 K by Zhang et al. [32] and 2.5 by Xu et al. [14]. The larger λ reported in this work indicates strengthening *vdW* bonding has stronger influence on CNT/CNT than those between GNR/*h*-BN and GNR/GNR. As shown in Fig. 5, separation distance has an inverted dependence on LJ parameter χ. As the LJ parameter χ increases, the *vdW* bonding between CNTs becomes stronger, which causes stronger interactions between the two CNTs and leads to shorter separation distance.

Although it is difficult to tune contact pressures directly via *vdW* bonding strength in practical applications, it can be achieved by applying external forces or pressures [33] through electron irradiation [34]. Dependence of thermal conductance on external force is shown in Fig. 6. The negative values represent pulling force which corresponds to scaling parameter χ <1. The positive values stand for pressing forces which is equivalent to situations where χ >1. The pressing forces will make the separation distance between CNTs shorter and the interaction between CNTs stronger, leading to better interfacial thermal conduction. The *G* increases from 28 pW/K to 94 pW/K by a factor of 3.4 in our work when the applied force varied from 0 to 9.6 nN compared to a factor of 4 increment with the same applied force variation in the work by Evans et al. [19]. Applied force can shorten the separation distance of the CNTs to enhance heat conduction. Meanwhile, applied force would deform the nanotubes from horizontal to ellipse, leading to more junction areas between the CNTs to strengthen the thermal conduction. In their work, the severe deformation in CNTs leads to significant junction area increase. In comparison, the CNTs have less deformations in this work which result in less enhancement of junction area correspondingly. In addition, deformation in individual CNT would suppress the thermal conductivity of CNT [35], thus the total interfacial thermal resistance would increase and *G* decreases accordingly. The deformation in CNTs has two aspects of influence on *G*.

Based on above discussions, applying external forces and adjusting the LJ coupling parameter χ have equivalent influences on thermal conductance. A synthesized figure for the relationship of applied force, χ and the final separation distance is depicted to help analyze the effect of applied force and LJ scaling parameter χ on the strength of *vdW* bonding and final separation distance between CNTs as shown in Fig. 7. The relationship between applied force and LJ scaling parameter is established through the value of thermal conductance. Since both adjustment of applied force and LJ scaling parameter can change the value of thermal conductance, the corresponding thermal conductance for a given LJ scaling parameter is obtained as displayed in Fig. 5. The applied force corresponding to the same value of thermal conductance can be obtained by linear difference with two adjacent values of thermal conductance and corresponding values of applied force as shown in Fig. 6. Thus the relationship between applied force and LJ scaling parameter is obtained as shown in Fig. 7. When LJ parameter χ is less than 1, the energy scale ε is reduced (the LJ parameter χ is changed by adjusting the energy scale ε correspondingly) to weaken the interactions between CNTs, *i.e.*, weaker *vdW* bonding will lead to larger separation distance. Accordingly, negative pulling forces enlarge the separation distance, which has the same effects with decreasing χ. When χ >1, which corresponds to the positive force, the interactions between two CNTs are strengthened and result in shorter separation distances. Accordingly, positive pressing forces would push two CNTs close to each other to reinforce the interaction between them. Thus the thermal conductance increases when LJ parameter χ >1 or CNTs are applied with pressure force.

The establishment of such relationship is important because it can be used as a guidance for modulating interfacial thermal conductance via mechanical force. In practical applications, there are various approaches to manipulate the contact pressures between adjacent materials, such as mechanical compression forces, laser irradiation, chemical functionalization and interlayer insertions. In this work, we altered the contact pressure by changing the interatomic forces and mechanical strength, which are relatively easy to achieve through numerical methods and can reasonably mimic the realistic conditions. It is worth noting that the latter approach can be directly replicated in the experimental studies, while the former method is limited to theoretical studies. On the micro level, applying force on two nano-structures could shorten the separation distance between the adjacent heterostructures to strengthen their interactions, and thus resulting in increased *G*. On the nanoscale level, when squeezing CNT bulk or powder materials, the volume would shrink and thermal conductivity would increase; but the increasing ranges of different materials are discrepant. The thermal conductance and separation distance between two molecules are explored with MD simulation, thus the thermal conductance and

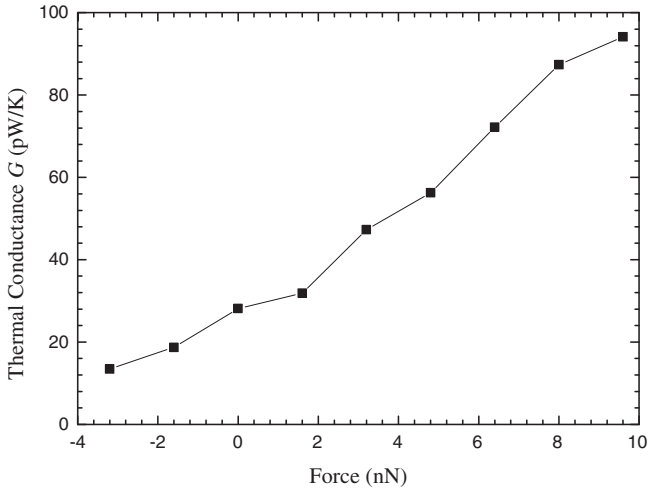

Fig. 6. Thermal conductance of the perpendicular stacked CNTs as a function of applied force. The negative and positive force values represent pulling and pressing forces individually, which corresponds to situations where χ <1 and χ >1.

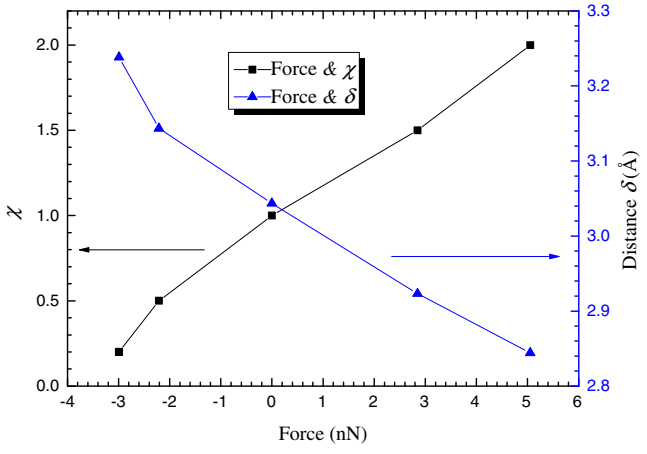

Fig. 7. Synthesized relationship of applied force, LJ parameter χ and the final separation distance δ between CNTs. The black solid line with square symbols describes force as a function of χ. And the blue solid line with triangle symbol represent force as a function of δ. (For interpretation of the references to colour in this figure legend, the reader is referred to the web version of this article.)

volume of CNT bulk or powder materials may be regulated via mechanical force. This method can also be applied on other interfacial thermal transport studies between film/wires or between film/substrate for comprehensively understanding the mechanisms in different physical models.

3.3. Effects of covalent organic linkers

Above-mentioned approaches of varying crossing angle, altering contact area, tuning the strength of *vdW* bonding and applying external force can enhance the interfacial thermal conductance, but the effects are limited. It is worth noting that the interaction modes between CNTs are van der Waals bonding in above cases. Another effective method to strengthen the thermal conduction between molecules is transforming the interatomic interaction from *vdW* bond to covalent bond. The thermal conductance between covalent structures are significantly higher than those between *vdW* structures [36]. The covalent interaction is orders of magnitude more conducive for interfacial phonon transport compared to *vdW* interactions. Previous work by Varshney et al. [20,37] provides a feasible approach to create covalent bonds between CNTs by using organic linkers to connect two CNTs. Covalent bonds are formed with both CNTs by the linker. In our work, hydrocarbon chain CH_2 is used to link two CNTs by covalent bonding interacted mode for studying interfacial thermal transport improvement.

Fig. 8 shows thermal conductance as a function of the CH_2 linker density (number of linkers per unit length). The thermal conductance can increase by a factor of 20 as the density varies from 0 to 2.5, indicating that the improvement of interfacial thermal conductance is remarkable by connecting the two CNTs with CH_2 linkers. However, as the density of CH_2 linkers increases beyond 2.5, the enhancement of interfacial thermal conductance decreases, *i.e.*, there is an optimum density for using CH_2 linkers to connect between CNTs. The effect of hydrocarbon CH_2 chain linkers on thermal conductance is multiple. Firstly, the CH_2 linkers form covalent bonds between two CNTs, which lead to prominent increase of thermal conductance. Ni et al. [38] reported that the interfacial thermal conductance between two CNTs increased significantly by HLK5 polymer functionalization of CNTs. However, the covalent bonds between CH_2 and the two CNTs will destroy the intrinsic structure of CNTs. As is known, the excellent thermal performance of CNT is due to the specific geometric construction. The formed covalent bonds produce defects in CNTs interface, which will affect thermal transport significantly [39]. Overlarge density of covalent bonds between CH_2 linkers and CNTs will undermine the intrinsic structure of CNT badly. And it was reported that the thermal conductivity of intrinsic CNT was suppressed with functionalization [38,40]. Thus the thermal resistance of individual CNT increase with CH_2 linkers. Besides, there are regions with defects along CNTs and these regions with defects will scatter different types of phonons. This leads to phonon spectra mismatch, which will reduce thermal transport between two CNTs. In this scenario, the heterostructure is considered to be composed with two parts, CNT-only and CNT-linker. In the processes of interfacial thermal energy dissipation, there are two channels that account for the heat transfer between CNTs. The first channel is through the linker, which is from one CNT to the linker, and the linker to the other CNT. The second channel is CNT-CNT only, since the CNT-CNT are still connected by van der Waals interactions and phonons can directly transmit through. Another possible factor for the decrease of interfacial thermal conductance at higher densities is that spitting distance between adjacent linkers may interfere with each other's transmission. And more CH_2 linkers would increase the thermal resistance between CNTs. In general, more CH_2 linkers will form more covalent bonds to reinforce thermal transport between CNTs [20,37], whereas the partial distortion in perfect CNT structures might introduce modification in phonon spectrum distribution and thus induce more thermal resistance inside CNTs and the mismatched phonon spectrums of local regions with defects on CNTs, interfered transmission by adjacent CH_2 linkers and resistance from CH_2 linkers increase thermal resistance at interface, thus the total resistance increases when the density is beyond 2.5, and the thermal conductance will decrease accordingly. In addition, when the number of linkers is small (less than 20), there are periodic linker structures between two parallel CNTs. If the number of linkers is increased to more than 20, the perfect periodic structures will be destroyed: as the density is high, the distance between adjacent linkers is not same for all adjacent linkers. For example, when the number of linkers is 25, there are 24 pairs of adjacent linkers. The distance of 8 pairs is about 0.25 nm, while the distance of rest 16 pairs is about 0.5 nm. This imperfect structure could be the partial reason for decreased thermal conductance at larger linker numbers. The result shown in Fig. 8 suggests that enhancement of thermal conductance at the interface between CNTs can be achieved through transforming *vdW* bonding to covalent interaction, *i.e.*, by introducing organic molecules to connect the interface.

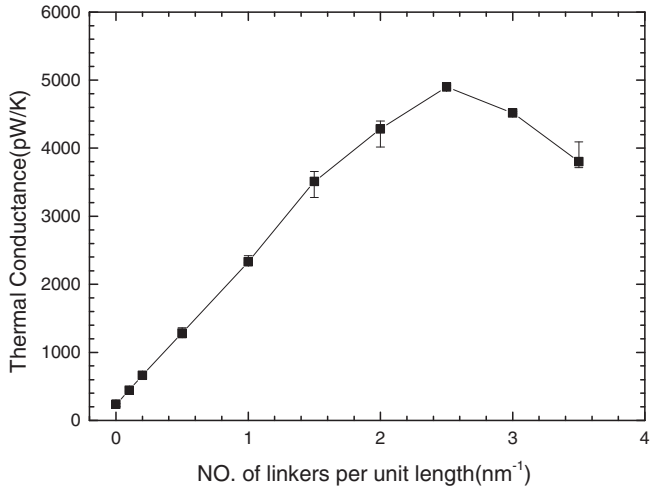

Fig. 8. Thermal conductance *G* as a function of linker number per unit length.

It is found in Fig. 8 that when the linker density is below 2.5, the increase in thermal conductance is nonlinear, and this nonlinear phenomenon is more obvious as the density increases. This nonlinear phenomenon is attributed to two main reasons: (1) the phonon transmission of CH_2 linkers at interface is influenced by adjacent CH_2 linkers. When the density is increased, the space between adjacent linkers is reduced, and then the CH_2 linkers are more strongly affected by neighboring CH_2 linkers, which leads to obvious nonlinear increase in thermal conductance at higher density. (2) The defects in carbon nanotubes at interface affect thermal conductance [37]. The regions with defects will cause severe phonon scatterings which result in larger phonon spectra mismatch between CNTs. As the number of CH_2 linkers is varied from 1 to 35, the defects in CNTs at the interface are increased significantly. Therefore, the nonlinear increase becomes more obvious at higher density of CH_2 linkers.

4. Conclusion

In summary, stacked CNTs are modeled to investigate thermal transport process at CNT/CNT interfaces with various crossing angle, contact area, *vdW* bonding strength, external force and number of hydrocarbon chain linkers. It is found that thermal conductance at the junction of two non-bonded CNTs decreases with

increasing crossing angle and decreasing contact area and increases with increasing strength of *vdW* bonding and applied force. Besides, tuning strength of *vdW* bonding and applying force on CNTs have similar effects on thermal conductance. A synthesized figure depicting the relationship of LJ scaling parameter, applied force and final separation distance between CNTs is used to analyze the effects of applied force and strength of van der Waals bonding on thermal conductance. To further enhance the interfacial thermal conductance, we transform the interaction between two CNTs into covalent bonding by adding hydrocarbon chain linkers at the junctions. The calculated thermal conductance increases significantly by a factor of 20, from 229 pW/K to 4901 pW/K. Opposing to previous report [20], it is found the calculated G does not increase monotonically with CH_2, *i.e.*, there is an optimal number of CH_2 linkers for the increase of thermal conductance.

Acknowledgements

The financial support from the National Natural Science Foundation of China (Nos. 51206124, 51428603 and 51576145) is gratefully acknowledged.

Reference

[1] S. Iijima, Helical microtubules of graphitic carbon, Nature 354 (6348) (1991) 56–58.
[2] P. Kim, L. Shi, A. Majumdar, P.L. McEuen, Thermal transport measurements of individual multiwalled nanotubes, Phys. Rev. Lett. 87 (21) (2001).
[3] M.J. Biercuk, M.C. Llaguno, M. Radosavljevic, J.K. Hyun, A.T. Johnson, J.E. Fischer, Carbon nanotube composites for thermal management, Appl. Phys. Lett. 80 (15) (2002) 2767.
[4] O. Breuer, U. Sundararaj, Big returns from small fibers: a review of polymer/carbon nanotube composites, Polym. Compos. 25 (6) (2004) 630–645.
[5] E.T. Thostenson, Z. Ren, T.-W. Chou, Advances in the science and technology of carbon nanotubes and their composites: a review, Compos. Sci. Technol. 61 (13) (2001) 1899–1912.
[6] Z. Han, A. Fina, Thermal conductivity of carbon nanotubes and their polymer nanocomposites: a review, Prog. Polym. Sci. 36 (7) (2011) 914–944.
[7] A. Moisala, Q. Li, I. Kinloch, A. Windle, Thermal and electrical conductivity of single-and multi-walled carbon nanotube-epoxy composites, Compos. Sci. Technol. 66 (10) (2006) 1285–1288.
[8] H.L. Zhang, J.F. Li, K.F. Yao, L.D. Chen, Spark plasma sintering and thermal conductivity of carbon nanotube bulk materials, J. Appl. Phys. 97 (11) (2005) 114310.
[9] C.W. Nan, G. Liu, Y. Lin, M. Li, Interface effect on thermal conductivity of carbon nanotube composites, Appl. Phys. Lett. 85 (16) (2004) 3549–3551.
[10] A.K. Vallabhaneni, B. Qiu, J. Hu, Y.P. Chen, A.K. Roy, X. Ruan, Interfacial thermal conductance limit and thermal rectification across vertical carbon nanotube/graphene nanoribbon-silicon interfaces, J. Appl. Phys. 113 (6) (2013) 064311.
[11] K. Bui, B.P. Grady, D.V. Papavassiliou, Heat transfer in high volume fraction CNT nanocomposites: effects of inter-nanotube thermal resistance, Chem. Phys. Lett. 508 (4–6) (2011) 248–251.
[12] P. Kapitza, The study of heat transfer in helium II, J. Phys. (USSR) 4 (1–6) (1941) 181–210.
[13] H. Zhong, J.R. Lukes, Interfacial thermal resistance between carbon nanotubes: molecular dynamics simulations and analytical thermal modeling, Phys. Rev. B 74 (12) (2006).
[14] Z. Xu, M.J. Buehler, Nanoengineering heat transfer performance at carbon nanotube interfaces, ACS Nano 3 (9) (2009) 2767–2775.
[15] Y. Chalopin, S. Volz, N. Mingo, Upper bound to the thermal conductivity of carbon nanotube pellets, J. Appl. Phys. 105 (8) (2009) 084301.
[16] J. Yang, S. Waltermire, Y. Chen, A.A. Zinn, T.T. Xu, D. Li, Contact thermal resistance between individual multiwall carbon nanotubes, Appl. Phys. Lett. 96 (2) (2010) 023109.
[17] M. Foygel, R. Morris, D. Anez, S. French, V. Sobolev, Theoretical and computational studies of carbon nanotube composites and suspensions: electrical and thermal conductivity, Phys. Rev. B 71 (10) (2005) 104201.
[18] L. Hu, A.J.H. McGaughey, Thermal conductance of the junction between single-walled carbon nanotubes, Appl. Phys. Lett. 105 (19) (2014) 193104.
[19] W.J. Evans, M. Shen, P. Keblinski, Inter-tube thermal conductance in carbon nanotubes arrays and bundles: effects of contact area and pressure, Appl. Phys. Lett. 100 (26) (2012) 261908.
[20] V. Varshney, S.S. Patnaik, A.K. Roy, B.L. Farmer, Modeling of thermal conductance at transverse CNT−CNT interfaces, J. Phys. Chem. C 114 (39) (2010) 16223–16228.
[21] R.N. Salaway, L.V. Zhigilei, Thermal conductance of carbon nanotube contacts: molecular dynamics simulations and general description of the contact conductance, Phys. Rev. B 94 (1) (2016) 014308.
[22] W. Hoover, Nonequilibrium molecular dynamics, Annu. Rev. Phys. Chem. 34 (1) (1983) 103–127.
[23] G.J. Hu, B.Y. Cao, Thermal resistance between crossed carbon nanotubes: molecular dynamics simulations and analytical modeling, J. Appl. Phys. 114 (22) (2013) 224308.
[24] S.J. Stuart, A.B. Tutein, J.A. Harrison, A reactive potential for hydrocarbons with intermolecular interactions, J. Chem. Phys. 112 (14) (2000) 6472.
[25] R. Saito, R. Matsuo, T. Kimura, G. Dresselhaus, M. Dresselhaus, Anomalous potential barrier of double-wall carbon nanotube, Chem. Phys. Lett. 348 (3) (2001) 187–193.
[26] S. Plimpton, Fast parallel algorithms for short-range molecular dynamics, J. Comput. Phys. 117 (1) (1995) 1–19.
[27] D.J. Evans, B.L. Holian, The Nose-Hoover thermostat, J. Chem. Phys. 83 (8) (1985) 4069.
[28] P.K. Schelling, S.R. Phillpot, P. Keblinski, Comparison of atomic-level simulation methods for computing thermal conductivity, Phys. Rev. B 65 (14) (2002).
[29] D.P. Sellan, E.S. Landry, J.E. Turney, A.J.H. McGaughey, C.H. Amon, Size effects in molecular dynamics thermal conductivity predictions, Phys. Rev. B 81 (21) (2010).
[30] Y. Yue, J. Zhang, X. Wang, Micro/nanoscale spatial resolution temperature probing for the interfacial thermal characterization of epitaxial graphene on 4H-SiC, Small 7 (23) (2011) 3324–3333.
[31] X. Tang, S. Xu, J. Zhang, X. Wang, Five orders of magnitude reduction in energy coupling across corrugated graphene/substrate interfaces, ACS Appl. Mater. Interfaces 6 (4) (2014) 2809–2818.
[32] J. Zhang, Y. Hong, Y. Yue, Thermal transport across graphene and single layer hexagonal boron nitride, J. Appl. Phys. 117 (13) (2015) 134307.
[33] S.N. Schiffres, K.H. Kim, L. Hu, A.J. McGaughey, M.F. Islam, J.A. Malen, Gas diffusion, energy transport, and thermal accommodation in single-walled carbon nanotube aerogels, Adv. Funct. Mater. 22 (24) (2012) 5251–5258.
[34] L. Sun, F. Banhart, A. Krasheninnikov, J. Rodriguez-Manzo, M. Terrones, P. Ajayan, Carbon nanotubes as high-pressure cylinders and nanoextruders, Science 312 (5777) (2006) 1199–1202.
[35] J. Ma, Y. Ni, S. Volz, T. Dumitrică, Thermal transport in single-walled carbon nanotubes under pure bending, Phys. Rev. Appl. 3 (2) (2015) 024014.
[36] P. De Andres, R. Ramírez, J.A. Vergés, Strong covalent bonding between two graphene layers, Phys. Rev. B 77 (4) (2008) 045403.
[37] V. Varshney, J. Lee, A.K. Roy, B.L. Farmer, Modeling of interface thermal conductance in longitudinally connected carbon nanotube junctions, J. Appl. Phys. 109 (8) (2011) 084913.
[38] Y. Ni, H. Han, S. Volz, T. Dumitrică, Nanoscale azide polymer functionalization: a robust solution for suppressing the carbon nanotube-polymer matrix thermal interface resistance, J. Phys. Chem. C 119 (22) (2015) 12193–12198.
[39] N. Kondo, T. Yamamoto, K. Watanabe, Phonon wavepacket scattering dynamics in defective carbon nanotubes, Jpn. J. Appl. Phys. 45 (36) (2006) L963–L965.
[40] S. Shenogin, A. Bodapati, L. Xue, R. Ozisik, P. Keblinski, Effect of chemical functionalization on thermal transport of carbon nanotube composites, Appl. Phys. Lett. 85 (12) (2004) 2229–2231.